Identification of Different Proteins Binding to Na, K-ATPase α1 in Lipopolysaccharide-Induced Acute Respiratory Distress Syndrome Cell Model by Proteomic Analysis

Xu-Peng Wen
Transplantation Center, the Third Xiangya Hospital, Central South University, Changsha, 410013, Hunan, China
Yue-Zhong Zhang
Clinical Medicine, Xiangya School of Medicine, Central South University, Changsha, 410083, China
He Huang
Hunan International Travel Health Care Center
Tao-Hua Liu
Clinical Medicine, Xiangya School of Medicine, Central South University, Changsha, 410083, China
Qi-Quan Wan (13548685542@163.com)
Transplantation Center, the Third Xiangya Hospital, Central South University, Changsha, 410013, Hunan, China

Research Article

Keywords: ARDS, lipopolysaccharide, proteomics, Na, K-ATPase α1, A549 cell.

Posted Date: July 9th, 2021

DOI: https://doi.org/10.21203/rs.3.rs-687826/v1

Abstract

Acute respiratory distress syndrome (ARDS) is characterized by refractory hypoxemia caused by accumulation of pulmonary fluid, which is related to inflammatory cell infiltration, impaired tight junction of pulmonary epithelium and impaired Na, K-ATPase function, especially Na, K-ATPase α1 subunit. Up until now, the pathogenic mechanism at the level of protein during lipopolysaccharide- (LPS-) induced ARDS remains unclear. Using an unbiased, discovery and quantitative proteomic approach, the discovery of differentially expressed proteins binding to Na, K-ATPase α1 between LPS-induced A549 cell and control-A549 group is of particular interest for the current study. These proteins may help the clinical diagnosis and facilitate the personalized treatment of ARDS. We screened these Na, K-ATPase α1 interacting proteins, carried out the related Gene Ontology (GO) and Kyoto Encyclopedia of Genes and Genomes (KEGG) analysis, and found evident phenomena of ubiquitination and deubiquitination, as well as the pathways related to autophagy. We also chose some of the differentiated expressing proteins with significant performance for further verification by liquid chromatography-tandem mass spectrometry (LC-MS/MS). Among proteins with rich abundance, there were several intriguing ones, including the deubiquitinase (OTUB1), the tight junction protein zonula occludens-1 (ZO-1), the scaffold protein in CUL4B-RING ubiquitin ligase (CRL4B) complexes (CUL4B) and the autophagy-related protein sequestosome-1 (SQSTM1). Protein-protein interaction network showed that there were 244 significantly enriched co-expression among 60 proteins in the group control-A549. while the group LPS-A549 showed 43 significant enriched interactions among 29 proteins. In conclusion, our quantitative discovery-based proteomic approach identified commonalities, and revealed targets related to the occurrence and development of ARDS, being the first study to investigate significant differences in Na, K-ATPase α1 interacting proteins between LPS-induced ARDS cell model and control-A549 cell.

1. Introduction

Acute respiratory distress syndrome (ARDS) is a potentially fatal clinical syndrome that occurs as a result of diversified pulmonary and extrapulmonary factors, characterized by excessive lung inflammatory response, impaired tight junction of pulmonary epithelium, decreased pulmonary gas exchange ability and reduced alveolar fluid clearance (AFC) of the lungs with consequent refractory hypoxemia.[1] Every year, over 3 million patients worldwide suffer from ARDS. 10% of intensive care unit (ICU) patients were admitted as a result of ARDS. With high morbidity and mortality, it is a hot spot in the field of intensive care and respiratory medicine.[2] Effective removal of excess edema fluid in the alveoli and maintenance of dry alveolar space are the main ways to relieve ARDS.[3]

Over the past decade, considerable work has been done for eliminating excessive accumulation of alveolar edema fluid to relieve ARDS and is still in progress. The apically-located epithelial Na^+ channel (ENaC) and sodium pump, namely Na, K-ATPase, on the basolateral surface of alveolar type Ⅱ epithelial cells (AT Ⅱ) mediated sodium ion transport is the main dynamic of AFC.[4–6] The imbalance of Na, K-ATPase will aggravate the formation of pulmonary edema by limiting Na^+ transport and destroying the alveolar barrier function.[7]

Na, K-ATPase, is a ubiquitous enzyme consisting of three subunits. Among them, α-subunit plays a key role and is the most important one in sodium-water transport as the main driving force of Na^+ and K^+ exchange in the lung to promote fluid clearance in the alveoli. There are four subtypes of α subunit, only α1 exists in lung.[8] Na, K-ATPase α1 carries several binding domains and functional domains.[9] Resolvin D1 can improve the expression of ENaC and Na, K-ATPase α1 protein and the activity of Na, K-ATPase enzyme through ALX/cAMP/PI3K pathway, thus improving the obstruction of pulmonary edema clearance caused by lipopolysaccharides (LPS).[10] However, researchers have not explored the systemic regulation mechanism of Na, K-ATPase. Similarly, a study has reported that Maresin1 can enhance the protein expression of Na, K-ATPase α1, which may be achieved through the ALX/PI3K/AKT/Nedd4-2 pathway.[6] Whereas, E3 ubiquitin ligase Nedd4-2 has no structural binding sites with Na, K-ATPase. Maresin1 could not increase Na, K-ATPase α1 level through increasing the phosphorylation of Nedd4-2 and its binding with 14-3-3 protein. The mechanism of Maresin1 regulating Na, K-ATPase α1 is not clear. Thus, investigating Na, K-ATPase α1-related pathway may provide new strategies and targets for ARDS treatment. But, a powerful tool to precisely and quantitatively detect changes in protein expression in response to ARDS is necessary.

Unbiased discovery and the quantitative proteomic approach, enabling relatively comprehensive global analyses, have been used for identifying novel biomarkers and regulatory signal networks in lung diseases including ARDS.[11–17] Studies identified some possible ARDS biomarkers, such as angiopoietin-2, surfactant proteins, glutathione, selectins, thrombomodulin, adenosine, Clara cell protein and many other biomarkers, which were reviewed before.[11,12,15–18] Several clinical trials failed since there was more than one pathway causing ARDS.[19–21] The research of ARDS biomarkers concerning several different fields, requiring a more comprehensive study method than traditional ones, thus non-targeted proteomics can be very suitable.

In the present study, we utilized LPS-induced human AT II cell line (A549) as a model of ARDS,[22–24] and detected the changes in the protein expression profiles of LPS-A549 group compared with control-A549 group and control-IgG group. Among them, protein complexes and protein interaction networks are essential mediators of most biological functions. Currently, the majority of studies on the composition of protein complexes are carried out by affinity purification mass spectrometry (AP-MS/MS), or by co-immunoprecipitation mass spectrometry (Co-IP-MS) for untransfected native samples, and present a static view of the system (Figs. 1 and 2) (free images were obtained from Aksomics). We employed affinity purification (AP) or co-immunoprecipitation (Co-IP) technology to separate endogenous or labeled bait proteins and the proteins interacting with them. Then, we used liquid chromatography-tandem mass spectrometry (LC-MS/MS) technology to identify and quantify these proteins, combined with Gene Ontology (GO) and Kyoto Encyclopedia of Genes and Genomes (KEGG) analysis, constructing the protein interaction network. Altogether, differential protein expression data may provide a valuable resource to reveal potential molecular targets for ARDS treatment.

2 Materials And Methods

2.1. Reagents

LPS (Escherichia coli serotype 055: B5), TCEP (tris (2-carboxyethyl) phosphine), IAA (iodoacetamide), PBS, C18 columns (3M), FA (Formic acid, LC-MS), TFA (Trifluoroacetic acid, HPLC) and 10% ammonium hydroxide were purchased from Sigma-Aldrich (St Louis, MO, USA); Na, K-ATPase α1 antibody was purchased from Proteintech, USA; ACN (Acetonitrile, LC-MS) and H2O (LC-MS) were purchased from J.T.Baker (PA, USA); Trypsin (sequence grade) was purchased from Promega (Madison, WI, USA); NP-40 (Nonidet P 40) and Ammonium bicarbonate (ABC) were purchased from Sangon Biotech (Shanghai, China); Dynabeads® Anti Rabbit IgG was purchased from Thermo Scientific (Rockford, USA); Normal rabbit IgG was purchased from Cell signaling technology (MA, USA); Protease inhibitor cocktail (PIC) was purchased from Kangchen Bio-tech (Shanghai, China).

2.2 Cell line and cell culture

A549 cell line was purchased from ATCC; A549 cells were seeded into plastic culture dishes at 1×106/cm2 and cultured in a humidified incubator (21 % O2, 5 % CO2, 37°C) in DMEM with 10% fetal bovine serum (FBS), 2 mM L-glutamine, 100 units/ml penicillin, and 100μg/ml streptomycin. For all experiments, cells were grown and maintained in six-well plates, and cells were serum deprived for 24 h prior to pretreatment with LPS at a concentration of 1 ug/ml for 12 h at 37°C.

2.3 Sample preparation

For all experiments, cells were grown and maintained in six-well plates without 10% FBS for 12 hours before the experiment started. Subsequent experiments were conducted on medium without 10% FBS. There were two groups: A: A549 cells, B: A549 cells + LPS (1μg/ml, cultured for 12h). ARDS was induced by LPS according to previous reports.[10] The proteins were detected by mass spectrometry, and the amount of protein was 4 mg. Na, K-ATPase α1 antibody was used to pull down the Na, K-ATPase α1 proteins in two groups of cells. These proteins were pulled down for label-free mass spectrometry to understand the binding and interacting protein, and then the protein of interest was selected for verification.

2.4 Sample lysis

(1) Just before being used, Mix PBSN (PBS, 1% NP-40) and Protease inhibitor cocktail (PIC) were pre-chilled at 4°C. (2) Add 1mL lysis buffer to cell pellet, mix well, and sonicate to dissolve with ice bath. (3) 14000 g, centrifuge 15min at 4°C, transfer the supernatant to a new EP tube and keep it on ice.

2.5 Co-IP

(1) For each sample, use 50μL anti-igG Dynabeads. Wash beads with 500μL PBSN and shake gently for 1min, then discard supernatant. Repeat 3 times. (2) Mix 2μg antibody or normal IgG with 200Î¼L PBSN, re-suspend the cleaned Dynabeads and shake 1h at 4°C slowly. (3) Wash out free antibody with 500μL PBSN and shake gently for 1min, then discard supernatant. Repeat 3 times. (4) Mix Dynabeads with sample lysate, shake 2h at 4°C slowly. Transfer the supernatant to new EP tube and store at -80°C. (5) Wash out unbinding proteins with 500μL PBSN and shake gently for 1min, then discard supernatant. Repeat 3 times. (6) Wash out NP-40, which is incompatible with LC-MS, with 500μL PBS and shake gently for 1min, then discard supernatant. Repeat 4 times. (7) Add 50μL 1% TFA to Dynabeads, incubate 10min at 37°C with highspeed shaking to elute binding proteins. Transfer supernatant to new load-binding EP tube. Repeat the elution step once, combine two elutions, and adjust to neutral pH with 10% ammonium hydroxide. Add 100μL ABC buffer for trypsin digest.

2.6 TCA precipitation (optional)

(1) Precipitate protein with 0.1% SDC and 10% TCA at 4°C for 2h. (2) Spin at top speed, wash pellets with pre-cold 80% acetone 3 times. (3) Re-dissolve protein with 100μL ABC buffer for tryptic digestion.

2.7 Tryptic digestion

Tryptic digestion was performed as described previously.[25] (1) Add 5mM TCEP to each sample, incubate and mix at 55°C for 10 min. (2) Add 10mM IAA after samples cooling down to room temperature, incubate in the dark for 15 min. (3) Re-suspend trypsin with re-suspension buffer to 0.5μg/μL and incubate at room temperature for 5 min. (4) Add 1μL trypsin solution to each sample. (5) Mix well and spin down, incubate at 37°C with Thermomixer for ~ 8 h or overnight, quench reaction with 1% TFA.

2.8 Peptide desalting for LC-MS/MS

Peptide desalting for LC-MS/MS was performed as described previously.[26] (1) Equilibrate C18tip column with 200 μL ACN. (2) Wash out ACN with 200μL 0.1% FA 2 times, discard the washout. (3) Load peptide solution to C18tip column, let the solution flow through the column slowly, and collect flow-through (A). (4) Repeat the peptide loading step once. (5) Wash column with 200μL 0.1% FA, discard the washout. (6) Elute peptide with 50μL 70% ACN, collect elution (B) with new EP tube. (7) Repeat the desalting step (up 6 steps) once more with flow-through (A). (8) Merge 2 elution (B), vacuum dry the elution under 4°C or RT. (9) Re-suspend peptide with 10μL 0.1% FA for LC-MS/MS analysis, or store peptide powder at -80°C.

2.9 LC-MS/MS

LC-MS/MS -based assays was performed as previously described with some minor alterations.[26,27] For each sample, ~ 1/2 peptide were separated and analyzed with a nano-UPLC (EASY-nLC1200) coupled to Q-Exactive mass spectrometry (Thermo Finnigan). Separation was performed using a reversed-phase column (100 μm, ID × 15 cm, Reprosil-Pur 120 C18-AQ, 1.9μm, Dr. Math). Mobile phases were H2O with 0.1 % FA, 2 % ACN (phase A) and 80 % ACN, 0.1 % FA (phase B). Separation of sample was executed with a 120 min gradient at 300 nL/min flow rate. Gradient B: 8 to 30 % for 92 min, 30 to 40 % for 20 min, 40 to 100 % for 2 min, 100 % for 2 min, 100 to 2 % for 2 min and 2 % for 2 min. Data dependent acquisition was performed in profile and positive mode with Orbitrap analyzer at a resolution of 70,000 (@200 m/z) and m/z range of 350–1600 for MS1; For MS2, the resolution was set to 17,500 with a dynamic first mass. The automatic gain control (AGC) target for MS1 was set to 1.0 E + 6 with max IT 100ms, and 5.0 E + 4 for MS2 with max IT 200ms. The top 10 most intense ions were fragmented by HCD with normalized collision energy (NCE) of 27%, and isolation window of 2 m/z. The dynamic exclusion time window was 20s.

2.10 MaxQuant database search

The MaxQuant computational platform was performed as described previously.[28] Raw MS files were processed with MaxQuant (Version 1.5.6.0). The protein sequence database (Uniprot_organism_2016_09) was downloaded from UNIPROT. This database and its reverse decoy were then searched against by MaxQuant software. Trypsin was set as specific enzyme with up to 3 miss cleavage; Oxidation [M] and Acetyl [protein N-term] were considered as variable modification (max number of modifications per peptide is 3), Carbamidomethyl [C] was set as fixed modification; Both peptide and protein FDR should be less than 0.01. Only unique & razor peptides were used for quantification. All the other parameters were reserved as default.

2.11 Quantification and class specific grouping

We performed proteomic profiling from target group and control group of A549 cells (Table 1) using the Co-IP and LC-MS/MS technology. In this study, the FDR of polypeptide and protein levels were all controlled at 0.01. And the difference multiple selection, identification and quantitative results were as follows: FCA value≥1 or FCA value≤-1, and the protein with unique peptide number ≥ 2 was defined as significant difference. Firstly, the corresponding background was deducted according to the IgG situation of each sample, then compare the two samples. Among them, test sample (T) means FCA value > 1 and simultaneously number of unique peptide number ≥ 2,control sample (C) means FCA value≤-1 and number of unique peptide number ≥ 2。T&C shows − 1 ≤ FCA value ≤ 1, or unique peptide number≤2.

Table 1
Sample grouping.

Sample ID	Tag	IP Condition
A549	IgG	IgG
	A549	Antibody
A549 LPS	IgG	IgG
	LPS	Antibody
The experiment was divided into two groups: A: A549 cells, B: A549 cells + LPS (1μg/ml, cultured for 12h)		

2.12 Bioinformatics Analysis

Enrichment of gene ontology (GO) terms was measured.[29] Further, pathway analysis for the differentially expressed genes (DEGs) was carried out by Kyoto Encyclopedia of Genes and Genomes (KEGG) tool which was performed by STRING analysis (https://string-db.org/).[30] The interactions of the DEGs were also determined by STRING.

2.13 Statistical Analysis

The normalized spectral count of protein in purification was performed as previously described.[31] It is defined as the ratio of the normalized spectral count of protein in purification with bait j, Ti,j, to the average normalized spectral count of that protein across the negative controls (user controls or selected CRAPome controls), Ci, calculated as F Ci,j= (Ti,j + α)/(Ci + α). The normalized spectral counts are computed as Ti,j = SCi,j/Nj, where the normalization factor is the sum over all proteins identified in the experiment with bait j, Nj=∑SCi,j. Similarly, the counts are normalized in each negative-control experiment x = 1...n, Ci,x = SCi,x/Nx, before the averaged normalized count across all n controls, Ci = 1/n∑Ci,x, is computed. A small background factor α is added to prevent division by 0, calculated as β/ave(Nx), where ave(Nx) is the average normalization factor across all n negative controls. The parameter β is by default set to 1. Statistical significance was set at a $P < 0.05$ (*), $P < 0.01$ (**) and $P < 0.001$ (***) according to the results of the two-sided Student's t test.

3 Results

3.1 Na, K-ATPase α1 antibody successfully pulled down the binding proteins of Na, K-ATPase α1 by Co-IP

To verify whether there are proteins that can bind to Na, K-ATPase α1, the total proteins were isolated from cell lysates and then detected by Western blot. A549 cells were divided into two groups: the control-A549 and LPS-A549 groups. The protein expression of Na, K-ATPase α1 was detected in both groups (both $p < 0.001$) (Fig. 3). Thus, we concluded that there were proteins that could interact with and bind to Na, K-ATPase α1 in both groups, from which we could start related proteomic analysis and identify exactly related proteins of Na, K-ATPase α1 in the future work.

3.2 Identification and quantification of different proteins between target group and control group

To identify and quantify the significant proteins, in this study, we performed that the total number of identified and quantitated proteins in this assay was 1598, and among them, there are 738 proteins after filtration and 89 differentially expressed proteins in the group LPS-A549 compared with control-A549

(Table 2). 698 significant proteins in the group Control-A549 compared with IgG-A549 and 478 significant proteins in the group LPS-A549 compared with IgG-LPS (Table 3)

Table 2
Experimental results and Statistics

Total number of peptides	Total number of protein (Group)	Number of proteins after filtration (Group)	Number of differentially expressed proteins
10841	1598	738	89

Table 3
Results info. Summary. Significant proteins

Group	#Significant
Control-A549—IgG-A549.T	698
Control-A549—IgG-A549.C	22
Control-A549—IgG-A549.T&C	660
LPS-A549—IgG-LPS.T	478
LPS-A549—IgG-LPS.C	17
LPS-A549—IgG-LPS.T&C	796
Note. Test enriched (T), control enriched (C), and none enriched (T&C)	

Respectively, Venn diagrams were then drawn to confirm the different proteins in the three comparisons, namely, LPS-A549 vs. control-A549 (Fig. 4), LPS-A549 vs. IgG-LPS (Figure S1) and control-A549 vs. IgG-A549 (Figure S2). Three parts of Venn diagram are corresponding to test enriched (T), control enriched (C), and none enriched (T&C). In the discovery phase, we identified that 29 proteins were enriched in the LPS-A549 group, 60 proteins were enriched in the Control-A549 group, and 649 proteins were co-enriched in both groups (Fig. 4). We ranked the proteins according to fold change in expression levels and listed the top 10 candidates of significantly up-or down-regulated proteins (Table 4). Also, we found that 738 proteins contained E3 ubiquitin ligase or its complex components: TRIP12, RNF21 and CUL4B, deubiquitinases UCHL1, EIF3F and OTUB1, tight junction protein TJP1, and multifunctional protein SQSTM1. Among them, UCHL1 and RNF213 only enriched in the control group, while CUL4B, TRIP12, EIF3F, TJP1, SQSTM1 and OTUB1 enriched in both groups, indicating that they are strongly bound to Na, K-ATPase α1. These analysis results suggested that the difference in proteomic profiling is reliable. In future work, we can select the proteins we are interested in to carry out some relevant verification.

Table 4
Top 10 up-or down-regulated proteins ranking by FC in LPS-A549 group vs. control-A549 group.

Rank	LPS-A549 vs Control-A549		
	Annotation	Alias	FC*
Up-regulated Proteins			
1	keratin 17	KRT17	3.20673671
2	dihydrolipoamide dehydrogenase	DLD	2.619500792
3	nicalin	NCLN	2.355100614
4	mutS homolog 2	MSH2	2.355100614
5	heterogeneous nuclear ribonucleoprotein H3 (2H9)	HNRNPH3	1.619500792
6	stearoyl-CoA desaturase (delta-9-desaturase)	SCD	1.619500792
7	LIM and SH3 protein 1	LASP1	1.451281189
8	coatomer protein complex, subunit beta 2 (beta prime)	COPB2	1.451281189
9	coiled-coil domain containing 86	CCDC86	1.355100614
10	solute carrier family 1 (neutral amino acid transporter), member 5	SLC1A5	1.355100614
Down-regulated Proteins			
1	ribosomal RNA processing 1 homolog B	RRP1B	-3.459431619
2	dolichyl-phosphate mannosyltransferase polypeptide 1	DPM1	-2.584962501
3	GDP dissociation inhibitor 2	GDI2	-2.321928095
4	nucleoporin 107kDa	NUP107	-2.321928095
5	talin 1	TLN1	-2.321928095
6	WD repeat domain 36	WDR36	-2.321928095
7	WD repeat domain 46	WDR46	-2.149102965
8	DEAH (Asp-Glu-Ala-Asp/His) box polypeptide 57	DHX57	-2.000000000
9	G1 to S phase transition 2	GSPT2	-2.000000000
10	nuclear factor of kappa light polypeptide gene enhancer in B-cells 2	NFKB2	-2.000000000
*FC = Fold Change			

3.3 GO & KEGG enrichment analysis of proteins interacting with Na, K-ATPase α1

To search for shared functions among genes, a common way is to incorporate the biological knowledge, by using Gene Ontology (GO) and Kyoto Encyclopedia of Genes and Genomes (KEGG) analysis, to identify predominant biological themes of a collection of genes.

One of the main uses of the GO/KEGG is to perform enrichment analysis on gene sets. For example, given a set of genes that are up-regulated under certain conditions, an enrichment analysis will find which GO/KEGG terms are over-represented (or under-represented) using annotations for that gene set.

3.3.1 GO enrichment

GO analysis (http://www.geneontology.org/) was applied to search for significantly enriched GO terms in areas of biological process (BP), cellular component (CC), and molecular function (MF). Prediction terms with P-value less than 0.05 were selected and ranked by gene count ((Count/Pop. Hits)/(List. Total/Pop. Total)) or enrichment score (log10(adjust p-value)).

According to the results of group Control-A549 vs. IgG-A549, 750 BP terms, 229 CC terms, and 204 MF terms were found enriched in class-specific test enriched (T) sample compared with control enriched (C) sample. Similarly, in line with the results of group LPS-A549 vs. IgG-LPS, 697 BP terms, 202 CC terms, and 177 MF terms were found enriched in T sample. These generally changed GO terms in T sample and classified by BP, CC, MF, and ranked by gene count and enrichment score (Fig. 5a and 5b) ($p < 1.0 \times 10^{-7}$ in all terms).

Nevertheless, for what we are concerned about the results of group LPS-A549 vs. Control-A549, only 2 BP terms, 0 CC terms, and 40 MF terms were found enriched in T sample compared with C sample (namely, 1 BP terms, 20 CC terms, and 15 MF terms were found enriched) (Fig. 6a and 6b). Intriguingly, almost all of the most enriched and meaningful BP terms were related to biosynthetic process in the LPS-A549 group, for instance, “thioester biosynthetic process (GO:0035384),” “acyl-CoA biosynthetic process (GO:0071616),” and only “ribosome biogenesis (GO:0042254)” in the Control-A549 group. Some more detailed data can be found in (Figure S3 and S4).In addition, we could find that DEGs in MF terms were mostly enriched in misfolded protein binding, double-strand/single DNA junction binding, formate-tetrahydrofolate ligase activity, uniporter activity, SUMO activating enzyme binding, single thymine insertion

binding, dinucleotide repeat insertion binding, nucleoside triphosphate adenylate kinase activity, ligase activity, forming carbon-nitrogen bonds and heteroduplex DNA loop binding (Fig. 6a).

The most enriched CC terms were primarily about the cell in only group control-A549 such as “90S pre-ribosome (GO:0030686),” “pre-ribosome (GO:0030684),” “melanosome (GO:0042470),” “pigment granule (GO:0048770),” and “small-subunit processsome (GO:0032040).”

As for GO MF terms ranked by either gene count or enrichment score, the mainly enriched terms were closely related to enzymatic activity and protein binding. Represented terms were “misfolded protein binding (GO:0051787),” “double-strand/single-strand DNA junction binding (GO:0000406),” “formate-tetrahydrofolate ligase activity (GO:0004329),” “SUMO activating enzyme activity (GO:0019948),” in the LPS-A549 group, and “ATP-dependent RNA helicase activity (GO:0004004),” and “ATPase activity (GO:0016887).” “ATPase activity, coupled (GO:0042623),” in the Control-A549 group.

3.3.2 KEGG pathway

KEGG is one of the databases commonly used for pathway studies. To analyze and identify the most important metabolic and signal transduction pathways involved in differentially expressed proteins, similar to GO analysis, we selected differentially expressed proteins for KEGG enrichment analysis, and the results demonstrated that the KEGG pathway was significantly enriched ($p.adjust < 0.05$). Pathways ($p.adjust < 0.05$) were selected and ranked by gene counts. Overall, in the group Control-A549 vs. IgG-A549, 689 differentially expressed proteins were involved in 23 KEGG pathways, like Ribosome, Spliceosome and Carbon metabolism. And in the group LPS-A549 vs. IgG-LPS, 478 differentially expressed proteins were involved in 29 KEGG pathways. The proteins were primarily enriched in RNA transport and Fatty acid metabolism. These pathways were listed in (Fig. 7a and 7b) and top 20 pathways were listed for up-regulated genes, respectively (Table S1). Conversely, in the group LPS-A549 vs. control-A549, there was no significant enriched signal pathways.

3.4 STRINGdb protein-protein interaction (PPI) analysis

To further examine the comprehensive information obtain from the identified protein data, the PPI network was analyzed. The network model was generated using the STRING website based on formation derived from 5 main sources: Genomic Context Predictions, High-throughput Lab Experiments, Co-Expression (Conserved), Automated Text mining, Previous Knowledge in Databases. A merged network is shown in (Figure S5 and S6), and, significant proteins annotation (show 50 if available) are shown in (Table S2 and S3). 738 proteins after filter were screened into the PPI network complex, which showed that there were 244 significant enriched interactions among 60 proteins in the group control-A549 (Fig. 8a). Moreover, in the group LPS-A549, it contained 43 significant enriched interactions among 29 proteins (Fig. 8b). Some explanations of protein-protein interaction links are shown (Fig. 8c).

3.5 Ubiquitination and de-ubiquitination enrichment related to OTUB1

In the analysis of protein mass spectrometry, OTUB1(known as a deubiquitinases) is of particular interest. OTUB1 belongs to the ovarian cancer proteases family. In this study, we found that Na, K-ATPase α 1 can bind to the deubiquitinase OTUB1 by protein mass spectrometry. Also, in the A549 cell group, GO analysis of Na, K-ATPase α1 interacting proteins showed significant enrichment of ubiquitination and deubiquitination, both were related to OTUB1. The enrichment items of ubiquitination and deubiquitination enrichment items are shown in (Table 5)

Table 5
The enrichment items of ubiquitination and deubiquitination by GO analysis

ID	Description	Gene ID
GO: 0016579	Protein deubiquitination	RHOA/SHMT2/PSMC6/PSMA7/PSMD12/PSMC5/PSMC3/PSMA6/PSMC2/RPS27A/PSMC4/UCHL1/PSMD3/EIF3F/PSMD
GO: 0031397	Negative regulation of protein ubiquitination	RPL23/HSPA1A/**OTUB1**/U2AF2/GTPBP4/RPS3/DNAJA1/RPS7/TRIP12
GO: 0031625	Ubiquitin protein ligase binding	RPL23/HSPD1/PA2G4/HSPA1A/RPS27A/EGFR/UCHL1/**OTUB1**/GPI/HSPA9/NDUFS2/YWHAZ/LRPPRC/RTN4/YWHAE/CUL
GO: 0044389	Ubiquitin-like protein ligase binding	RPL23/HSPD1/PA2G4/HSPA1A/RPS27A/EGFR/UCHL1/**OTUB1**/GPI/HSPA9/NDUFS2/YWHAZ/LRPPRC/RTN4/YWHAE/CUL
GO: 0070646	Protein modification by small protein removal	RHOA/SHMT2/PSMC6/PSMA7/PSMD12/PSMC5/PSMC3/PSMA6/PSMC2/RPS27A/PSMC4/UCHL1/PSMD3/EIF3F/PSMD
GO: 1903321	Negative regulation of protein modification by small protein conjugation or removal	RPL23/HSPA1A/**OTUB1**/U2AF2/GTPBP4/RPS3/DNAJA1/RPS7/TRIP12
GO: 0033183	Negative regulation of histone ubiquitination	**OTUB1**/TRIP12
GO: 1901314	Regulation of histone H2A K63-linked	**OTUB1**/TRIP12
GO: 1901315	Negative regulation of histone H2A K63-linked	**OTUB1**/TRIP12

Otub1 is marked in red, CUL4B is marked in green, SQSTM1 is marked in blue.

3.6 Na, K-ATPase α 1 interacts with SQSTM1 and CUL4B through Co-IP and western blot verification

Protein ubiquitination is a key step in the ubquitin-proteasome degradation pathway, and autophagy plays an indispensable role in maintaining cell homeostasis, clearing excess proteins and organelles, apoptosis, metabolism and senescence. We next selected the autophagy-related protein (SQSTM1) and the scaffold protein in CUL4B-RING ubiquitin ligase (CRL4B) complexes (CUL4B) from the significantly differentially expressed proteins for verification. Western blot assay followed after the Co-IP by Na, K-ATPase α1 antibody showed that both of SQSTM1 and CUL4B were positive (Fig. 9), which indicated that there was a close relationship between Na, K-ATPase α1 and proteins related to autophagy and ubiquitination pathway. In all, further studies are needed to verify these results.

IP: Na, K-ATPase murine monoclonal antibody, abcam,ab2872. **Na, K-ATPase α1 group**, WB: 1:1000, 100KD. Second antibody: Goat anti-Mouse IgG (Light Chain Specific), HRP Conjugated, S003, 1:5000. **SQSTM1 group**, WB: SQSTM1 rabbit polyclonal antibody, Proteintech, 18420-1, 1:10000, 62KD; Second antibody: Mouse anti-Rabbit IgG (Light Chain specific), HRP Conjugated, S006, 1:5000. **CUL4B group**, WB: CUL4B rabbit polyclonal antibody, Immunoway, YM5188, 1:1000, 110KD; Second antibody: Mouse anti-Rabbit IgG (Light Chain specific), HRP Conjugated, S006, 1:5000.62KD.

4. Discussion

ARDS is characterized by refractory hypoxemia due to infiltration of inflammatory cells and accumulation of lung water due to impaired Na, K-ATPase function and impaired tight junction of lung epithelium.[32] Despite advances in intensive care, it is associated with a high in-hospital mortality rate of approximately 40% .[33] Severe ARDS patients had a mortality rate of 63.9%.[34] Yet there is no effective drug treatment approved by Food and Drug Administration.[35] Moreover, few biomarkers can be used to predict the onset and progression of ARDS, to stratify the risk factors, or to predict prognosis.[36] The poor efficacy of traditional drugs may be related to the complicated pathogenic factor of ARDS.[2]

The most common causes of ARDS are bacterial pneumonia and sepsis, wherein Gram-negative bacteria are a prominent cause. LPS, the major constituent of the outer membrane of all Gram-negative bacteria, can easily cause the injury of epithelial cells along with resident alveolar macrophages in the airway,

thereby further resulting in a cascade of events including production of cytokines and chemokines, recruitment of neutrophils, monocytes and lymphocytes into the alveolar space and finally lead to ARDS.[37,38]

Proteomic methods can not only study the whole set of proteins of ARDS, and find out the key targets as the entry point of drug treatment, but also verify the drugs that may be effective in the treatment of ARDS, and study the possible mechanism of its intervention in the treatment of ARDS.[11,39] Although the application of proteomics technology in the pathogenesis of ARDS has just begun, its great potential in deepening the understanding of protein expression patterns, discovering new damage mediators and developing new therapeutic drugs has emerged.[40] Whereas, there are several ways, not just one, that cause ARDS when researchers focused on their limited specialized areas. Therefore, the traditional methods to find biomarkers are too limited, and proteomic research should be applied.

Na, K-ATPase α1 plays an important role in the regulation of fluid volume under various physiological and pathological conditions of ARDS. To our knowledge, this study is the first to determine the binding proteins of Na, K-ATPase α1 in ARDS by proteomic technologies. Several reviews have introduced and summarized the detailed technologies and methods of non-targeted proteomics.[12,16,41–45]

Our quantitative discovery-based proteomic approach identified commonalities as well as significant differences in the binding proteins of Na, K-ATPase α1 between A549 cells and LPS-induced A549 cells. Identification and validation of these proteins in ARDS patients are thus warranted, and strategies aimed to enhance these related pathways could form effective preventive measures or treatment options for ARDS patients. Before the experiment started, we found that Na, K-ATPase α 1 antibody successfully pulled down the binding proteins of Na, K-ATPase α 1 by Co-IP. Next, using proteomic analysis, we identified 1598 proteins. Of them, 89 were differentially expressed proteins (Table 2 and Fig. 4) between LPS-A549 cells and Control-A549 cells. We utilized PPI network analysis to select PPI and gene co-expression proteins that were linked to Na, K-ATPase α1. Furthermore, we conducted function and pathway analysis to seek biological pathways that may have an impact on ARDS.

Intriguingly, although protein concentration was not significantly increased in LPS-induced A549 cells, the protein expression profiles of the LPS-A549 group were significantly different from those of the controls with 29 up-regulated and 60 down-regulated proteins in LPS-A549 compared to control-A549 (Fig. 4). The present study highlights the ability of proteomic analysis to detect differential proteins in an A549 cell model of ARDS induced by LPS. And these proteins are expected to play specific roles in the pathogenesis of ARDS and may serve as useful biomarkers or potential therapeutic targets.

We screened these proteins interacted with Na, K-ATPase α1, and carried out the related GO/KEGG analysis. According to the GO analysis, we found that almost all of the most enriched and meaningful BP terms were related to biosynthetic process in the LPS-A549 group. The mainly enriched terms were closely related to enzymatic activity and protein binding. KEGG analysis showed that the proteins were primarily enriched in RNA transport and Fatty acid metabolism. The PPI network was built on the binding proteins that was analyzed by STRING website. We observed that there were 43 significant enriched interactions among 29 proteins in the LPS-A549 group. Besides, we found that there were obvious ubiquitination and deubiquitination phenomena, as well as the pathways related to autophagy.

Based on these results, we chose some proteins with expression levels that were significantly expressed for further verification by LC-MS/MS. Among the most expressed proteins, there were several intriguing proteins, including the deubiquitinase (OTUB1), the tight junction protein zonula occludens-1 (ZO-1), the scaffold protein in CUL4B-RING ubiquitin ligase (CRL4B) complexes (CUL4B) and the autophagy-related protein SQSTM1.

Ubiquitination is a type of protein post-translational modification.[46] Ubiquitination and deubiquitination ensure the stability of cell and body physiological function, which attaches great significance to the study of this dynamic process. Our GO analysis of Na, K-ATPase α1 interaction protein showed that ubiquitination and deubiquitination were significantly enriched, and both were related to OTUB1(Table 5). OTUB1, known as a deubiquitinases, can protect the protein from degradation and belongs to the ovarian cancer proteases family. Zhu D et al. found OTUB1 as a deubiquitinating enzyme that influences cancer immunosuppression via regulation of PD-L1 stability and may be a potential therapeutic target for cancer immunotherapy.[47] Mulas et al. found that OTUB1 was a potent novel regulator of dendritic cells (DCs) during infectious and inflammatory diseases.[48] Zhang W et al. found that OTUB1 performed as a molecular indicator of poor prognosis in digestive cancers, regulated the infiltration of tumor immunocytes, and exerted a significant influence on apoptosis and autophagy.[49] Our study found that LPS reduced the expression of OTUB1, which may act directly with Na, K-ATPase α1. Therefore, LPS may decrease the level of Na, K-ATPase α1 to lessen its protection by decreasing OTUB1. Combined with the previous conclusion, we speculate that up-regulating OTUB1 can protect Na, K-ATPase α1 from E3 ubiquitin ligase degradation, thus increasing Na, K-ATPase abundance and enzyme activity. More studies are needed to confirm whether OTUB1 can be a therapeutic site for ARDS in the future.

Lung permeability is determined by intercellular junctions such as gap junctions, adhesion junctions, and tight junctions. Tight junction is one of the important components of capillary-alveolar barrier, which plays an important role in reducing lung water production and stabilizing lung microenvironment.[50] ZO-1, a tight junction protein, regulates signal transduction, transcription, and cellular communication.[51,52] The down-regulation of its expression or activity can affect the formation of tight junctions between cells. Ni JJ et al. found that plasma ZO-1 proteins appear to be a valuable prognostic biomarker for the severity of sepsis and a predictor of 30-day mortality for patients with sepsis.[53] Li C et al. found that upregulating ZO-1/occludin/claudin-1 expression mitigates the inflammatory response and maintains intestinal barrier function in sepsis, providing a good experimental basis for its clinical treatment of sepsis.[54] And Lee TJ et al. found that ZO-1 on the exotoxin LPS of *P. aeruginosa*-induced diseases could be critical in the development of novel therapeutics.[55] It is interesting that, Na, K-ATPase β1 promotes the expression of key proteins such as ZO-1, ZO-2, occludin and claudin-18 in tight junction complex and reduces the production of lung water.[56] Ouabain, a specific inhibitor of Na, K-ATPase α1, induced the decrease of Na, K-ATPase α1/β1 in canine renal epithelial cells, and then induced the degradation of claudin-2, claudin-4, occludin and ZO-1 through EGFR-cSrc-ERK1/2 signaling pathway.[57] In our study, the level of ZO-1 mRNA in lung tissue of ARDS rats induced by LPS was significantly lower than that in control group.[58] Accordingly, we speculate that increasing the level of Na, K-

ATPase α1/β1 may enhance the tight junction of lung epithelium and reduce the production of lung water. The follow-up experiments are needed to verify our theory .

CUL4B, which acts as a scaffold protein in CUL4B-RING ubiquitin ligase (CRL4B) complexes, participates in a variety of biological processes, including embryonic development, cell cycle progression, DNA damage response, chromatin remodeling, and signaling transduction.[59] Li Y et al. suggested that in the development and progression of diffuse large B-cell lymphoma, CUL4B may act as a useful biomarker and a novel therapeutic target.[60] Song Y et al. reported that CUL4B functions to restrict TLR-triggered inflammatory responses through regulating the AKT-GSK3β pathway.[61] Our proteomic results show that CUL4B may bind to Na, K-ATPase α1 (Fig. 9), and the therapeutic target site of ARDS may extend to the effect of Na, K-ATPase α1 on CUL4B in subsequent studies.

SQSTM1, also known as sequestosome-1, is a multifunctional protein and is known as an autophagy protein that is destined for autophagic turnover by regulating the protein aggregates formation and facilitating the degradation of cargo protein through the process of autophagy.[62] SQSTM1 regulates multiple signaling pathways by binding to different proteins to form important signaling centers in cells.[63] SQSTM1 is involved in ubiquitin-proteasome and autophagy-lysosome degradation processes, and is an important regulatory molecule connecting ubiquitinated proteins to autophagy mechanism.[62] Liu Y et al. revealed that the relationship between Na, K-ATPase and autophagy-lysosome pathway requires the involvement of α1 subunit, and Na, K-ATPase α1 and AMPK may act as the “on” and “off” switch of autophagy pathway.[64] More importantly, Na, K-ATPase can be degraded through the ubiquitin-proteasome pathway and the autophagy-lysosome pathway. Autophagy defects can lead to SQSTM1 accumulation and induce cell stress and disease. In our study, we found that Na, K-ATPaseα1 could bind to SQSTM1 by protein profiling, which was verified by endogenous protein interaction analysis (Fig. 9). Consequently, the decrease of SQSTM1 mRNA expression may be helpful to reduce the transport of polyubiquitinated Na, K-ATPase α1 to autophagy-lysosome system for degradation. In summary, few studies have been conducted on the degradation pathways of Na, K-ATPase and autophagy protein SQSTM1, but the effect of their interaction on the abundance and enzyme activity of Na, K-ATPase α1, the improvement of lung water removal ability of alveolar cells, and the improvement of the prognosis of ARDS is worth extensive attention and discussion in the future.

Consideration differentially expressed proteins as biomarkers for ARDS have provided valuable insight into the pathogenesis. This is a new hope of identifying new biomarkers for prediction, prognostication, and diagnosis of ARDS.

Nevertheless, one of the limitations of this study is that the significant expression of these proteins occurred in LPS induced ARDS A549 cells model. We need to design a further study to investigate whether these changes also present in ARDS animal model.

5. Conclusion

In summary, using a quantitative discovery-based proteomic approach, this study identified commonalities as well as significant differences in protein expression profiles of ARDS cells model. Notably, the development of ARDS is related to many pathways, including autophagy lysosomal pathway, ubiquitination and deubiquitination, inflammatory response pathway, and pulmonary epithelial tight junction-related pathway. Based on this, we could roughly screen the important proteins and pathways related to the progression of ARDS, and propose possible therapy of extractive proteins including OTUB1, ZO-1, CUL4B and SQSTM1. However, it remains to be determined whether we can find some targets related to the occurrence and development of ARDS from these pathways. These key proteins still need to be tested using a large quantity of clinical specimens, and to be analyzed and validated in combination with the individual conditions of clinical patients. Further well-designed studies developing diagnostic panels and therapeutic targets based on these aberrantly expressed proteins and exploring the roles of these proteins that were most beneficial to ARDS are needed.

ASSOCIATED CONTENT

Supporting Information

Supplementary data related to this article can be found in Tables S1-4 and Figures S1-6.

Supporting Table S1. Top 20 up-regulated KEGG pathway analysis; Supporting Table S2. Results of group Control-A549–IgG-A549. Significant proteins annotation (show 50 if available); Supporting Table S3. Results of group LPS-A549–IgG-LPS. Significant proteins annotation (show 50 if available); Supporting Table S4. Abbreviations used in this study

Supporting Figure S1. Venn diagram of the different proteins in control-A549 vs. IgG-A549; Supporting Figure S2. Venn diagram of the different proteins in LPS-A549 vs. IgG-LPS; Supporting Figure S3. Enriched GO items of < C > in Control-A549 vs. IgG-A549. top axis is log10(adjust p-value), bottom axis is gene count; Supporting Figure S4. Enriched GO items of < C > in LPS-A549 vs. IgG-LPS. top axis is log10(adjust p-value), bottom axis is gene count; Supporting Figure S5. Control-A549–IgG-A549-STRINGdb-T-1; Supporting Figure S6. LPS-A549–IgG-LPS-STRINGdb-T-1

AUTHOR INFORMATION

Corresponding Author: **Qiquan Wan**, Transplantation Center, the Third Xiangya Hospital, Central South University, Changsha, 410013, Hunan, China. Tel: +86-731-88618312; E-mail:13548685542@163.com

Authors

XuPeng Wen [1] , Transplantation Center, the Third Xiangya Hospital, Central South University,Changsha, 410013, Hunan, China. E-mail: wxpwy1216@163.com.

YueZhong Zhang, Clinical Medicine, Xiangya School of Medicine, Central South University, Changsha, 410083, China.

He Huang, Hunan International Travel Health Care Center, Changsha 410001, Hunan, China.

TaoHua Liu, Clinical Medicine, Xiangya School of Medicine, Central South University, Changsha, 410083, China.

Abbreviations

ARDS: Acute respiratory distress syndrome;

ALI: Acute lung injury;

ICU: Intensive care unit;

LC-MS/MS: Liquid chromatography-tandem mass spectrometry;

AP-MS/MS: Affinity purification mass spectrometry;

Co-IP-MS: co-immunoprecipitation mass spectrometry;

AT II: Alveolar type II epithelial cells;

LPS: Lipopolysaccharide;

ENaC: Apically-located epithelial Na + channel;

A549: Human non-small cell lung cancer cell line/Human AT II cell line;

AFC: Alveolar fluid clearance;

GO: Gene Ontology;

KEGG: Kyoto Encyclopedia of Genes and Genomes;

Declarations

AUTHOR INFORMATION

Corresponding Author: **Qiquan Wan**, Transplantation Center, the Third Xiangya Hospital, Central South University, Changsha, 410013, Hunan, China. Tel: +86-731-88618312; E-mail:13548685542@163.com

Authors

XuPeng Wen[1], Transplantation Center, the Third Xiangya Hospital, Central South University，Changsha, 410013, Hunan, China. E-mail: wxpwy1216@163.com.

YueZhong Zhang, Clinical Medicine, Xiangya School of Medicine, Central South University, Changsha, 410083, China.

He Huang, Hunan International Travel Health Care Center, Changsha 410001, Hunan, China.

TaoHua Liu, Clinical Medicine, Xiangya School of Medicine, Central South University, Changsha, 410083, China.

Acknowledgements

This work was support by the Science and Technology Department of Hunan Province, China (grant 2020JJ4851). The authors thank KangChen Bio-Tech, Shanghai, China, for their technical support for the sequencing works.

Authors' contributions

Design and conduct of the study: QiQuan Wan. Collection of the data: XuPeng Wen. Management, analysis and interpretation of the data: XuPeng Wen and QiQuan Wan. Manuscript preparation: XuPeng Wen. Critical revision and approval of the manuscript: All authors.

Funding

This work was support by the Science and Technology Department of Hunan Province, China (grant 2020JJ4851).

Competing interests

The authors declare that they have no conflicts of interest financial or nonfinancial related to the content of this article.

Ethics approval and consent to participate

Not applicable.

References

1. Griffiths, M. J. D. *et al.* Guidelines on the management of acute respiratory distress syndrome[J]. *BMJ Open Respir Res*, **6** (1), e000420 https://doi.org/10.1136/bmjresp-2019-000420 (2019).
2. Fan, E., Brodie, D. & Slutsky, A. S. Acute Respiratory Distress Syndrome: Advances in Diagnosis and Treatment[J]. *JAMA*, **319** (7), 698–710 https://doi.org/10.1001/jama.2017.21907 (2018).
3. Force, A. D. T. *et al.* Acute respiratory distress syndrome: the Berlin Definition[J]. *JAMA*, **307** (23), 2526–2533 https://doi.org/10.1001/jama.2012.5669 (2012).
4. Matthay, M. A. & Zemans, R. L. The acute respiratory distress syndrome: pathogenesis and treatment[J]. *Annu Rev Pathol*, **6**, 147–163 https://doi.org/10.1146/annurev-pathol-011110-130158 (2011).
5. Vadasz, I. & Sznajder, J. I. Gas Exchange Disturbances Regulate Alveolar Fluid Clearance during Acute Lung Injury[J]. *Front Immunol*, **8**, 757 https://doi.org/10.3389/fimmu.2017.00757 (2017).
6. Zhang, J. L. *et al.* Maresin1 stimulates alveolar fluid clearance through the alveolar epithelial sodium channel Na,K-ATPase via the ALX/PI3K/Nedd4-2 pathway[J]. *Lab Invest*, **97** (5), 543–554 https://doi.org/10.1038/labinvest.2016.150 (2017).
7. Laffey, J. G. & Matthay, M. A. Fifty Years of Research in ARDS. Cell-based Therapy for Acute Respiratory Distress Syndrome. Biology and Potential Therapeutic Value[J]. *Am J Respir Crit Care Med*, **196** (3), 266–273 https://doi.org/10.1164/rccm.201701-0107CP (2017).
8. Cui, X. & Xie, Z. Protein Interaction and Na/K-ATPase-Mediated Signal Transduction[J]., **22** (6), https://doi.org/10.3390/molecules22060990 (2017).
9. Suhail, M. & Na, K-A-T-P. Ubiquitous Multifunctional Transmembrane Protein and its Relevance to Various Pathophysiological Conditions[J]. *J Clin Med Res*, **2** (1), 1–17 https://doi.org/10.4021/jocmr2010.02.263w (2010).
10. Wang, Q. *et al.* Resolvin D1 stimulates alveolar fluid clearance through alveolar epithelial sodium channel, Na,K-ATPase via ALX/cAMP/PI3K pathway in lipopolysaccharide-induced acute lung injury[J]. *J Immunol*, **192** (8), 3765–3777 https://doi.org/10.4049/jimmunol.1302421 (2014).
11. Levitt, J. E. & Rogers, A. J. Proteomic study of acute respiratory distress syndrome: current knowledge and implications for drug development[J]. *Expert Rev Proteomics*, **13** (5), 457–469 https://doi.org/10.1586/14789450.2016.1172481 (2016).
12. Norman, K. C. *et al.* Proteomics: Clinical and research applications in respiratory diseases[J]., **23** (11), 993–1003 https://doi.org/10.1111/resp.13383 (2018).
13. Bojkova, D. *et al.* Proteomics of SARS-CoV-2-infected host cells reveals therapy targets[J]. *Nature*, **583** (7816), 469–472 https://doi.org/10.1038/s41586-020-2332-7 (2020).
14. Usami, M. & Mitsunaga, K. Proteomic analysis and in vitro developmental toxicity tests for mechanism-based safety evaluation of chemicals[J]. *Expert Rev Proteomics*, **8** (2), 153–155 https://doi.org/10.1586/epr.11.16 (2011).
15. Janz, D. R. & Ware, L. B. Biomarkers of ALI/ARDS: pathogenesis, discovery, and relevance to clinical trials[J]. *Semin Respir Crit Care Med*, **34** (4), 537–548 https://doi.org/10.1055/s-0033-1351124 (2013).
16. Bhargava, M. *et al.* Application of clinical proteomics in acute respiratory distress syndrome[J]. *Clin Transl Med*, **3** (1), 34 https://doi.org/10.1186/s40169-014-0034-1 (2014).
17. Xu, X. F. *et al.* Mass Spectrometry-based Proteomics in Acute Respiratory Distress Syndrome: A Powerful Modality for Pulmonary Precision Medicine[J]. *Chin Med J (Engl)*, **129** (19), 2357–2364 https://doi.org/10.4103/0366-6999.190669 (2016).
18. Janga, H. *et al.* Site-specific and endothelial-mediated dysfunction of the alveolar-capillary barrier in response to lipopolysaccharides[J]. *J Cell Mol Med*, **22** (2), 982–998 https://doi.org/10.1111/jcmm.13421 (2018).
19. Matthay, M. A., Mcauley, D. F. & Ware, L. B. Clinical trials in acute respiratory distress syndrome: challenges and opportunities[J]. *Lancet Respir Med*, **5** (6), 524–534 https://doi.org/10.1016/S2213-2600(17)30188-1 (2017).
20. Briel, M. *et al.* Higher vs lower positive end-expiratory pressure in patients with acute lung injury and acute respiratory distress syndrome: systematic review and meta-analysis[J]. *JAMA*, **303** (9), 865–873 https://doi.org/10.1001/jama.2010.218 (2010).
21. Sauler, M., Bazan, I. S. & Lee, P. J. Cell Death in the Lung: The Apoptosis-Necroptosis Axis[J]. *Annu Rev Physiol*, **81**, 375–402 https://doi.org/10.1146/annurev-physiol-020518-114320 (2019).
22. Sporty, J. L., Horalkova, L. & Ehrhardt, C. In vitro cell culture models for the assessment of pulmonary drug disposition[J]. *Expert Opin Drug Metab Toxicol*, **4** (4), 333–345 https://doi.org/10.1517/17425255.4.4.333 (2008).
23. Ren, H., Birch, N. P. & Suresh, V. An Optimised Human Cell Culture Model for Alveolar Epithelial Transport[J]. *PLoS One*, **11** (10), e0165225 https://doi.org/10.1371/journal.pone.0165225 (2016).
24. Rocco, P. R. M. & Nieman, G. F. ARDS: what experimental models have taught us[J]. *Intensive Care Med*, **42** (5), 806–810 https://doi.org/10.1007/s00134-016-4268-9 (2016).
25. Masuda, T., Tomita, M. & Ishihama, Y. Phase transfer surfactant-aided trypsin digestion for membrane proteome analysis[J]. *J Proteome Res*, **7** (2), 731–740 https://doi.org/10.1021/pr700658q (2008).
26. Wang, Z. *et al.* A liquid chromatography-tandem mass spectrometry (LC-MS/MS)-based assay to profile 20 plasma steroids in endocrine disorders[J]. *Clin Chem Lab Med*, **58** (9), 1477–1487 https://doi.org/10.1515/cclm-2019-0869 (2020).
27. Li, J. & Zhu, H. J. Liquid Chromatography-Tandem Mass Spectrometry (LC-MS/MS)-Based Proteomics of Drug-Metabolizing Enzymes and Transporters[J]., **25** (11), https://doi.org/10.3390/molecules25112718 (2020).

28. Tyanova, S., Temu, T. & Cox, J. The MaxQuant computational platform for mass spectrometry-based shotgun proteomics[J]. *Nat Protoc*, **11** (12), 2301–2319 https://doi.org/10.1038/nprot.2016.136 (2016).
29. Xie, C. *et al.* Characterization of the global transcriptome for Pyropia haitanensis (Bangiales, Rhodophyta) and development of cSSR markers[J]. *BMC Genomics*, **14**, 107 https://doi.org/10.1186/1471-2164-14-107 (2013).
30. Liu, F. *et al.* High-abundance mRNAs in Apis mellifera: comparison between nurses and foragers[J]. *J Insect Physiol*, **57** (2), 274–279 https://doi.org/10.1016/j.jinsphys.2010.11.015 (2011).
31. Morris, J. H. *et al.* Affinity purification-mass spectrometry and network analysis to understand protein-protein interactions[J]. *Nat Protoc*, **9** (11), 2539–2554 https://doi.org/10.1038/nprot.2014.164 (2014).
32. Luyt, C. E. *et al.* Pulmonary infections complicating ARDS[J]. *Intensive Care Med*, **46** (12), 2168–2183 https://doi.org/10.1007/s00134-020-06292-z (2020).
33. Bellani, G. *et al.* Epidemiology, Patterns of Care, and Mortality for Patients With Acute Respiratory Distress Syndrome in Intensive Care Units in 50 Countries[J]. *JAMA*, **315** (8), 788–800 https://doi.org/10.1001/jama.2016.0291 (2016).
34. Wan, Q. *et al.* Acute respiratory distress syndrome in kidney transplant recipients[J]. *Intensive Care Med*, **41** (2), 373–374 https://doi.org/10.1007/s00134-014-3590-3 (2015).
35. Standiford, T. J. & Ward, P. A. Therapeutic targeting of acute lung injury and acute respiratory distress syndrome[J]. *Transl Res*, **167** (1), 183–191 https://doi.org/10.1016/j.trsl.2015.04.015 (2016).
36. Barnett, N. & Ware, L. B. Biomarkers in acute lung injury–marking forward progress[J]. *Crit Care Clin*, **27** (3), 661–683 https://doi.org/10.1016/j.ccc.2011.04.001 (2011).
37. Zhao, J. *et al.* Lysophosphatidic acid receptor 1 antagonist ki16425 blunts abdominal and systemic inflammation in a mouse model of peritoneal sepsis[J]. *Transl Res*, **166** (1), 80–88 https://doi.org/10.1016/j.trsl.2015.01.008 (2015).
38. Crosby, L. M. & Waters, C. M. Epithelial repair mechanisms in the lung[J]. *Am J Physiol Lung Cell Mol Physiol*, **298** (6), L715–731 https://doi.org/10.1152/ajplung.00361.2009 (2010).
39. Meyer, N. J. & Calfee, C. S. Novel translational approaches to the search for precision therapies for acute respiratory distress syndrome[J]. *Lancet Respir Med*, **5** (6), 512–523 https://doi.org/10.1016/S2213-2600(17)30187-X (2017).
40. Lynn, H. *et al.* Genomic and Genetic Approaches to Deciphering Acute Respiratory Distress Syndrome Risk and Mortality[J]. *Antioxid Redox Signal*, **31** (14), 1027–1052 https://doi.org/10.1089/ars.2018.7701 (2019).
41. Aebersold, R. & Mann, M. Mass spectrometry-based proteomics[J]. *Nature*, **422** (6928), 198–207 https://doi.org/10.1038/nature01511 (2003).
42. Bowler, R. P., Ellison, M. C. & Reisdorph, N. Proteomics in pulmonary medicine[J]., **130** (2), 567–574 https://doi.org/10.1378/chest.130.2.567 (2006).
43. Lam, E. & Dos Santos, C. C. Advances in molecular acute lung injury/acute respiratory distress syndrome and ventilator-induced lung injury: the role of genomics, proteomics, bioinformatics and translational biology[J]. *Curr Opin Crit Care*, **14** (1), 3–10 https://doi.org/10.1097/MCC.0b013e3282f42211 (2008).
44. Bowler, R. P. *et al.* Proteomic analysis of pulmonary edema fluid and plasma in patients with acute lung injury[J]. *Am J Physiol Lung Cell Mol Physiol*, **286** (6), L1095–1104 https://doi.org/10.1152/ajplung.00304.2003 (2004).
45. Wen, X. P., Zhang, Y. Z. & Wan, Q. Q. Non-targeted proteomics of acute respiratory distress syndrome: clinical and research applications[J]. *Proteome Sci*, **19** (1), 5 https://doi.org/10.1186/s12953-021-00174-y (2021).
46. Wu, H. Q., Baker, D. & Ovaa, H. Small molecules that target the ubiquitin system[J]. *Biochem Soc Trans*, **48** (2), 479–497 https://doi.org/10.1042/BST20190535 (2020).
47. Zhu, D. *et al.* Deubiquitinating enzyme OTUB1 promotes cancer cell immunosuppression via preventing ER-associated degradation of immune checkpoint protein PD-L1[J]. *Cell Death Differ*, https://doi.org/10.1038/s41418-020-00700-z (2020).
48. Mulas, F. *et al.* The deubiquitinase OTUB1 augments NF-kappaB-dependent immune responses in dendritic cells in infection and inflammation by stabilizing UBC13[J]. *Cell Mol Immunol*, https://doi.org/10.1038/s41423-020-0362-6 (2020).
49. Zhang, W. & Qiu, W. OTUB1 Recruits Tumor Infiltrating Lymphocytes and Is a Prognostic Marker in Digestive Cancers[J]. *Front Mol Biosci*, **7**, 212 https://doi.org/10.3389/fmolb.2020.00212 (2020).
50. Wittekindt, O. H. Tight junctions in pulmonary epithelia during lung inflammation[J]. *Pflugers Arch*, **469** (1), 135–147 https://doi.org/10.1007/s00424-016-1917-3 (2017).
51. Zhang, J. *et al.* Cardiomyocyte Expression of ZO-1 Is Essential for Normal Atrioventricular Conduction but Does Not Alter Ventricular Function[J]. *Circ Res*, **127** (2), 284–297 https://doi.org/10.1161/CIRCRESAHA.119.315539 (2020).
52. Schwayer, C. *et al.* Mechanosensation of Tight Junctions Depends on ZO-1 Phase Separation and Flow[J]., **179** (4), 937–952918 https://doi.org/10.1016/j.cell.2019.10.006 (2019).
53. Ni, J. *et al.* Plasma ZO-1 proteins predict the severity and outcome of sepsis: A prospective observational study[J]. *Clin Chim Acta*, **510**, 691–696 https://doi.org/10.1016/j.cca.2020.09.003 (2020).
54. Chen, L. *et al.* Tong-fu-li-fei decoction exerts a protective effect on intestinal barrier of sepsis in rats through upregulating ZO-1/occludin/claudin-1 expression[J]. *J Pharmacol Sci*, **143** (2), 89–96 https://doi.org/10.1016/j.jphs.2020.02.009 (2020).
55. Lee, T. J., Choi, Y. H. & Song, K. S. The PDZ motif peptide of ZO-1 attenuates Pseudomonas aeruginosa LPS-induced airway inflammation[J]. *Sci Rep*, **10** (1), 19644 https://doi.org/10.1038/s41598-020-76883-9 (2020).

56. Lin, X. *et al.* beta1-Na(+),K(+)-ATPase gene therapy upregulates tight junctions to rescue lipopolysaccharide-induced acute lung injury[J]. *Gene Ther*, **23** (6), 489–499 https://doi.org/10.1038/gt.2016.19 (2016).
57. Rincon-Heredia, R. *et al.* Ouabain induces endocytosis and degradation of tight junction proteins through ERK1/2-dependent pathways[J]. *Exp Cell Res*, **320** (1), 108–118 https://doi.org/10.1016/j.yexcr.2013.10.008 (2014).
58. Wan, Q. Q., Wu, D. & Ye, Q. F. Candidate Genes as Biomarkers in Lipopolysaccharide-Induced Acute Respiratory Distress Syndrome Based on mRNA Expression Profile by Next-Generation RNA-Seq Analysis[J]. Biomed Res Int, 2018, 2018: 4384797. doi:10.1155/2018/4384797
59. Liu, X. *et al.* The CUL4B-miR-372/373-PIK3CA-AKT axis regulates metastasis in bladder cancer[J]., **39** (17), 3588–3603 https://doi.org/10.1038/s41388-020-1236-1 (2020).
60. Li, Y. *et al.* CUL4B regulates autophagy via JNK signaling in diffuse large B-cell lymphoma[J]., **18** (4), 379–394 https://doi.org/10.1080/15384101.2018.1560718 (2019).
61. Song, Y. *et al.* CUL4B negatively regulates Toll-like receptor-triggered proinflammatory responses by repressing Pten transcription[J]. *Cell Mol Immunol*, **18** (2), 339–349 https://doi.org/10.1038/s41423-019-0323-0 (2021).
62. Vishnupriya, S. *et al.* Autophagy markers as mediators of lung injury-implication for therapeutic intervention[J]. *Life Sci*, **260**, 118308 https://doi.org/10.1016/j.lfs.2020.118308 (2020).
63. Lamark, T., Svenning, S. & Johansen, T. Regulation of selective autophagy: the p62/SQSTM1 paradigm[J]. *Essays Biochem*, **61** (6), 609–624 https://doi.org/10.1042/EBC20170035 (2017).
64. Liu, Y. *et al.* Autosis is a Na+,K+-ATPase-regulated form of cell death triggered by autophagy-inducing peptides, starvation, and hypoxia-ischemia[J]. *Proc Natl Acad Sci U S A*, **110** (51), 20364–20371 https://doi.org/10.1073/pnas.1319661110 (2013).

Figures

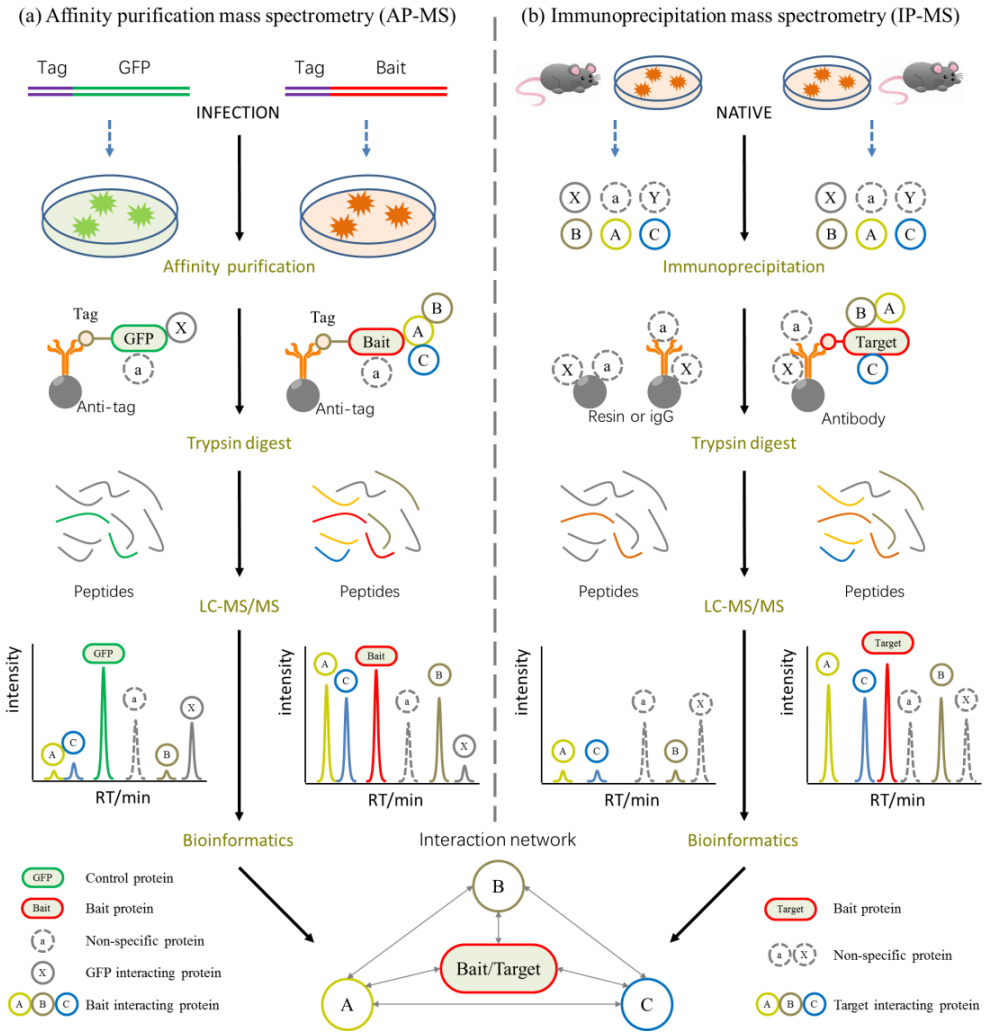

Figure 1

The workflow of AP-MS (IP-MS) technology. Using this approach with no IP-level antibodies are available against the target protein. Target protein(bait) is co-expressed with affinity tag and forms a complex with the endogenous components, then purified with immobilized tag affinity protein dynabeads and identified with LC-MS/MS after extensively washing off unspecifically bound proteins.

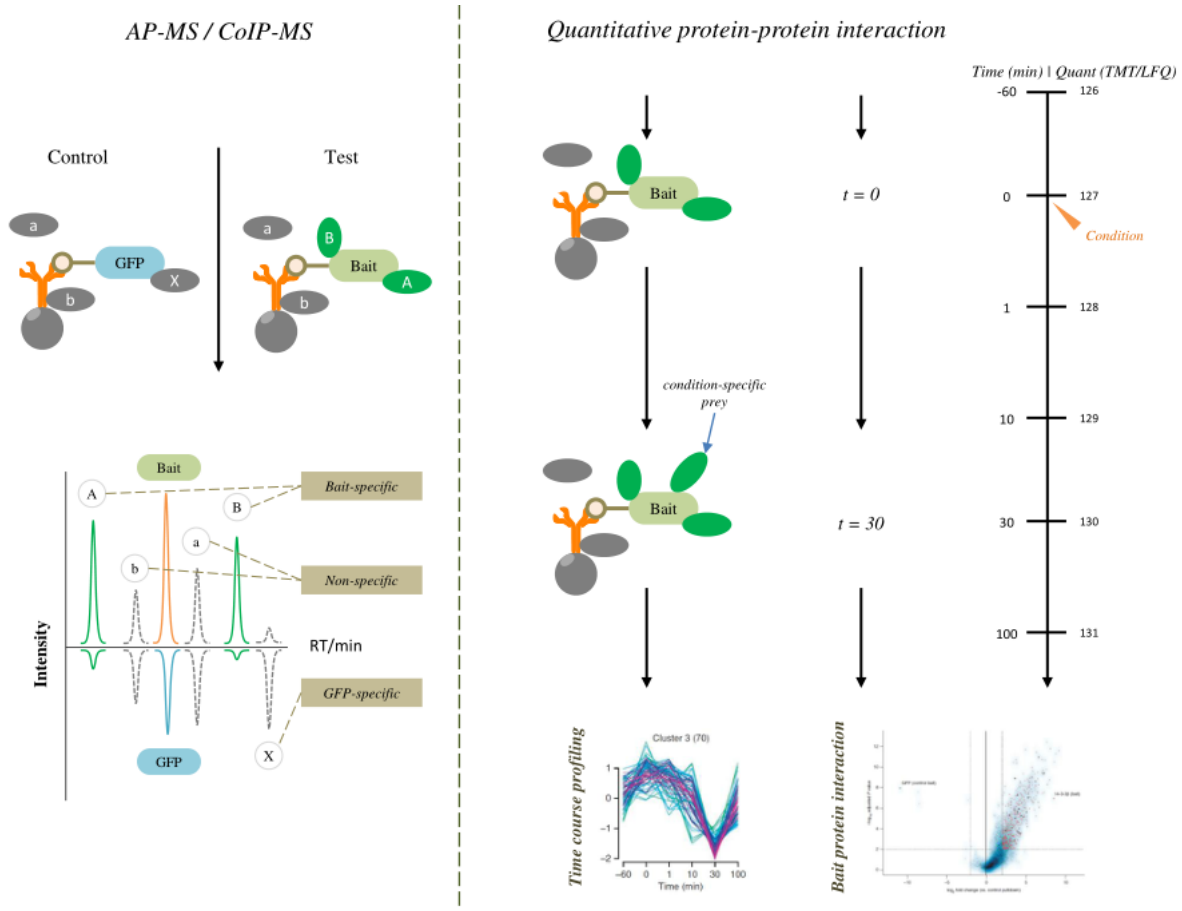

Figure 2

Procedure summary of Co-IP-MS techniques. Using this approach with IP-level antibodies are available against the target protein. For untransfected sample, protein complex is affinity captured from native cell lysates by an immobilized antibody that specifically recognizes an epitope of teh target (bait) protein. The co-isolated protein complex is washed extensively to remove unspecifically bound proteins and is subsequently eluted from the resin prior to protein identification by mass spectrometry.

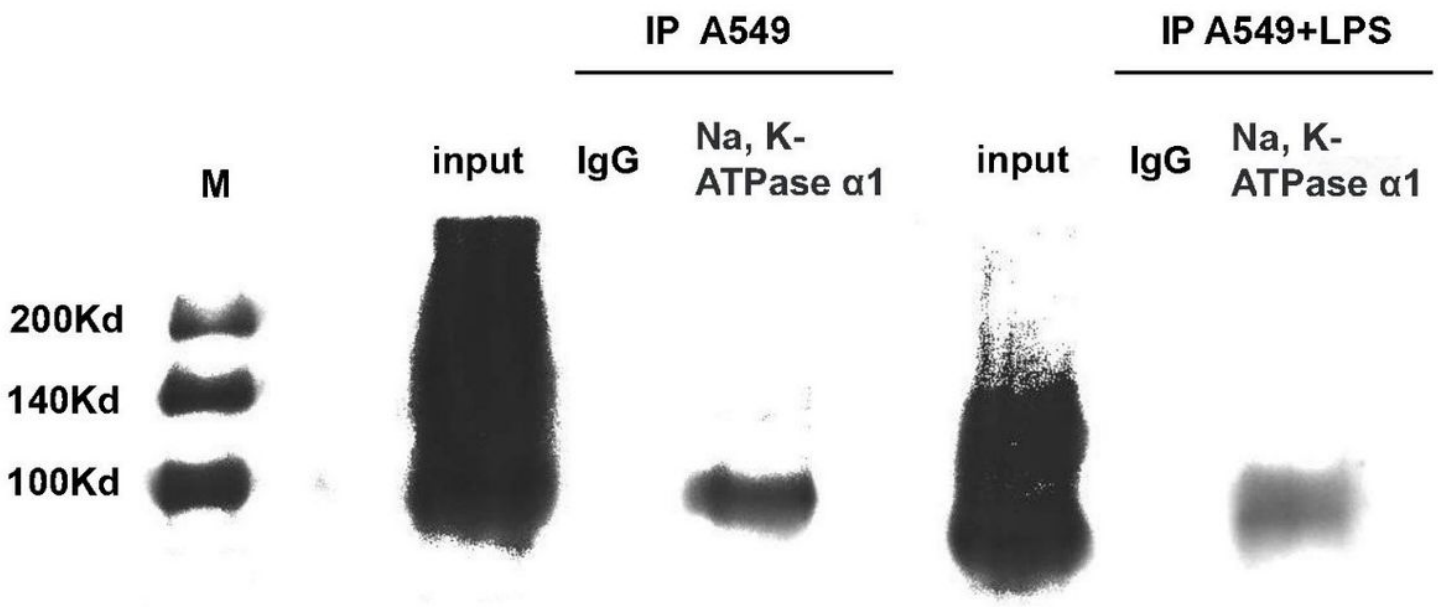

Figure 3

The binding proteins of Na, K-ATPase α1 in A549 group and A549+LPS group. The binding proteins of Na, K-ATPase α1 was detected in both groups using Co-IP assay followed by Western blot ($P < 0.001$). Proteins in whole-cell lysate were used as a positive control (input). ATP1A1: the gene name of Na, K-ATPase α1.

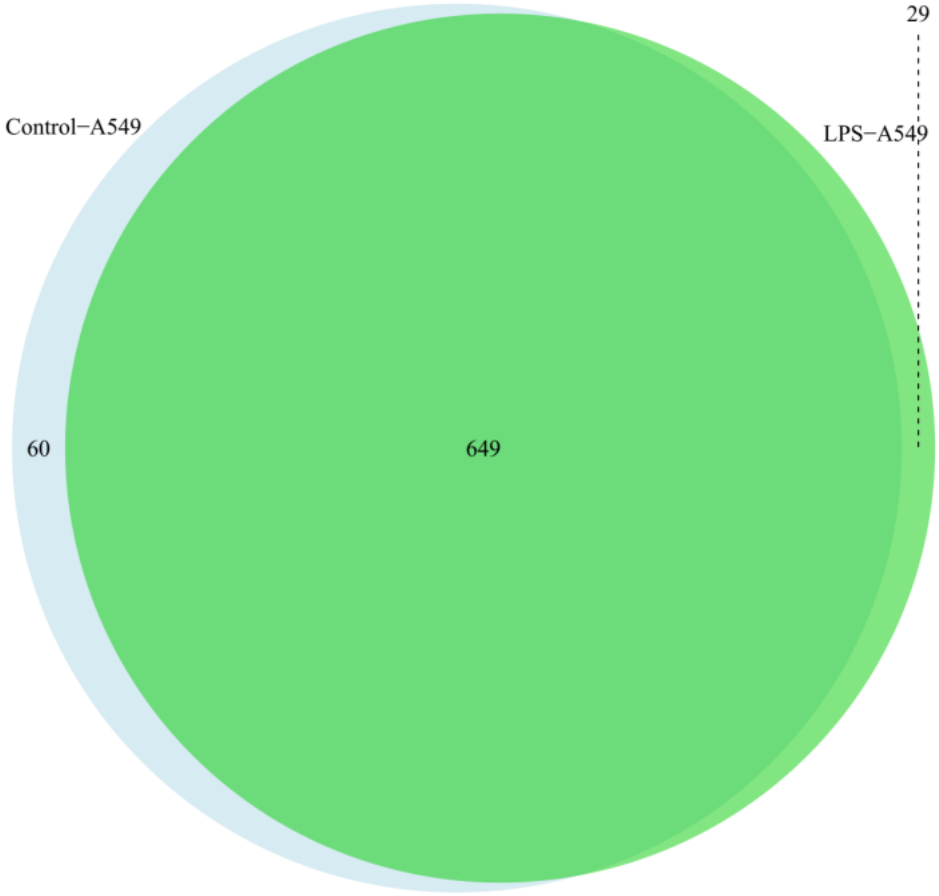

Figure 4

Venn diagram of the different proteins in LPS-A549 vs. control-A549. The green part represents proteins enriched in LPS-A549; The light blue represents proteins enriched in A549; The middle part is the protein identified by both of them.

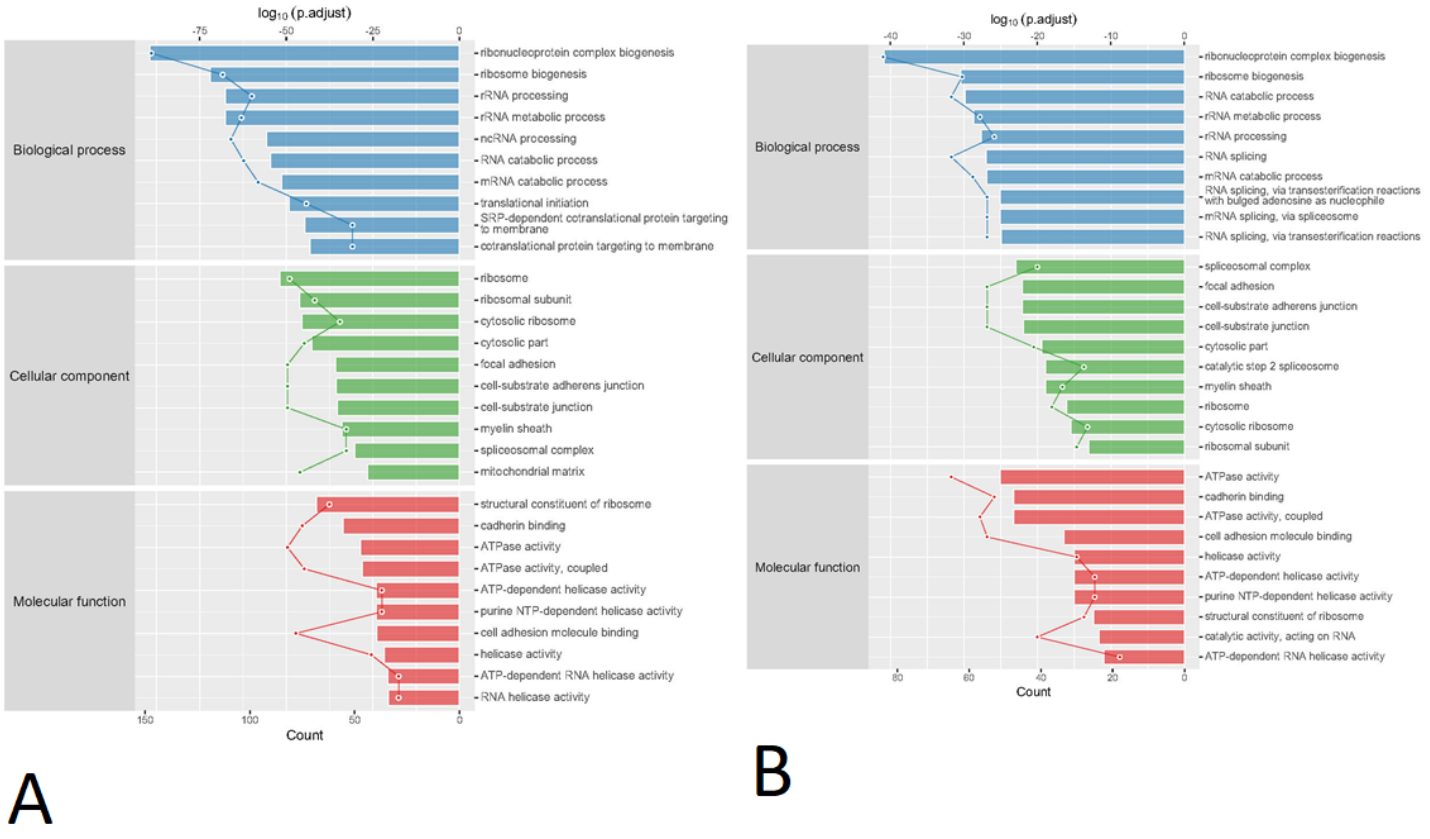

Figure 5

a. Enriched GO items of < T > in Control-A549 vs. IgG-A549. top axis is log10 (adjust p-value), bottom axis is gene count. b. Enriched GO items of < T > in LPS-A549 vs. IgG-LPS. top axis is log10(adjust p-value), bottom axis is gene count.

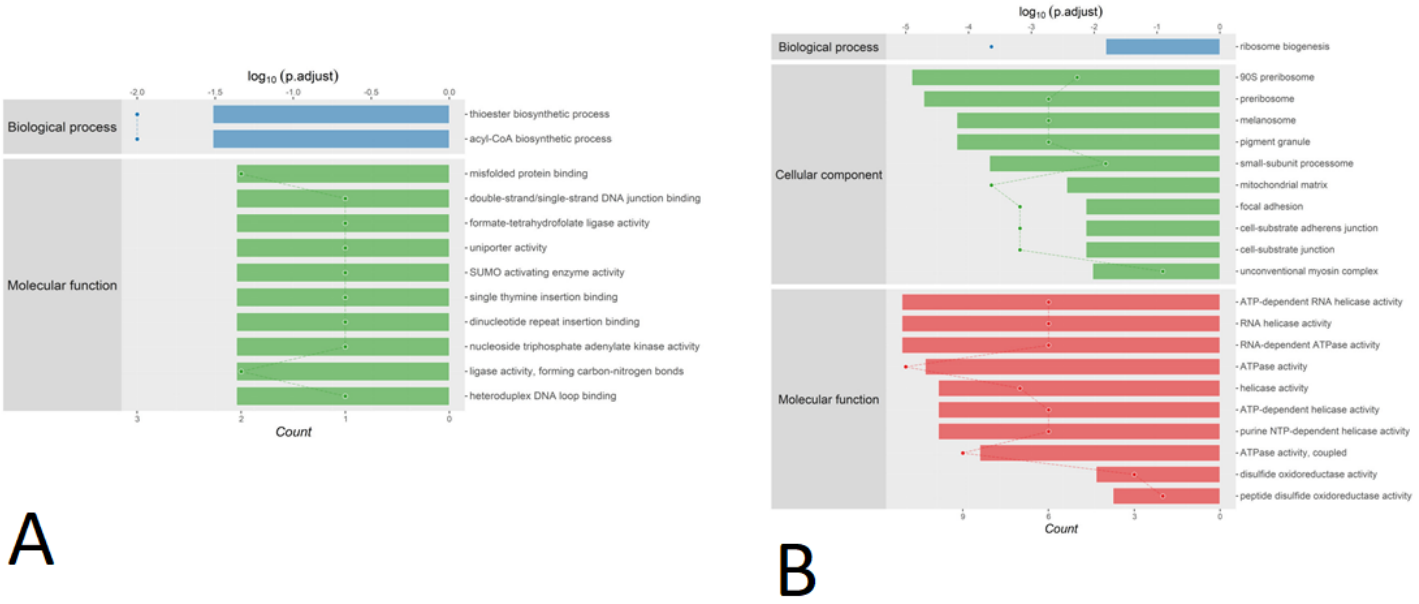

Figure 6

a. Enriched GO items of < T > in LPS-A549 vs. Control-A549. top axis is log10 (adjust p-value), bottom axis is gene count. b. Enriched GO items of < C > in LPS-A549 vs. Control-A549. top axis is log10 (adjust p-value), bottom axis is gene count.

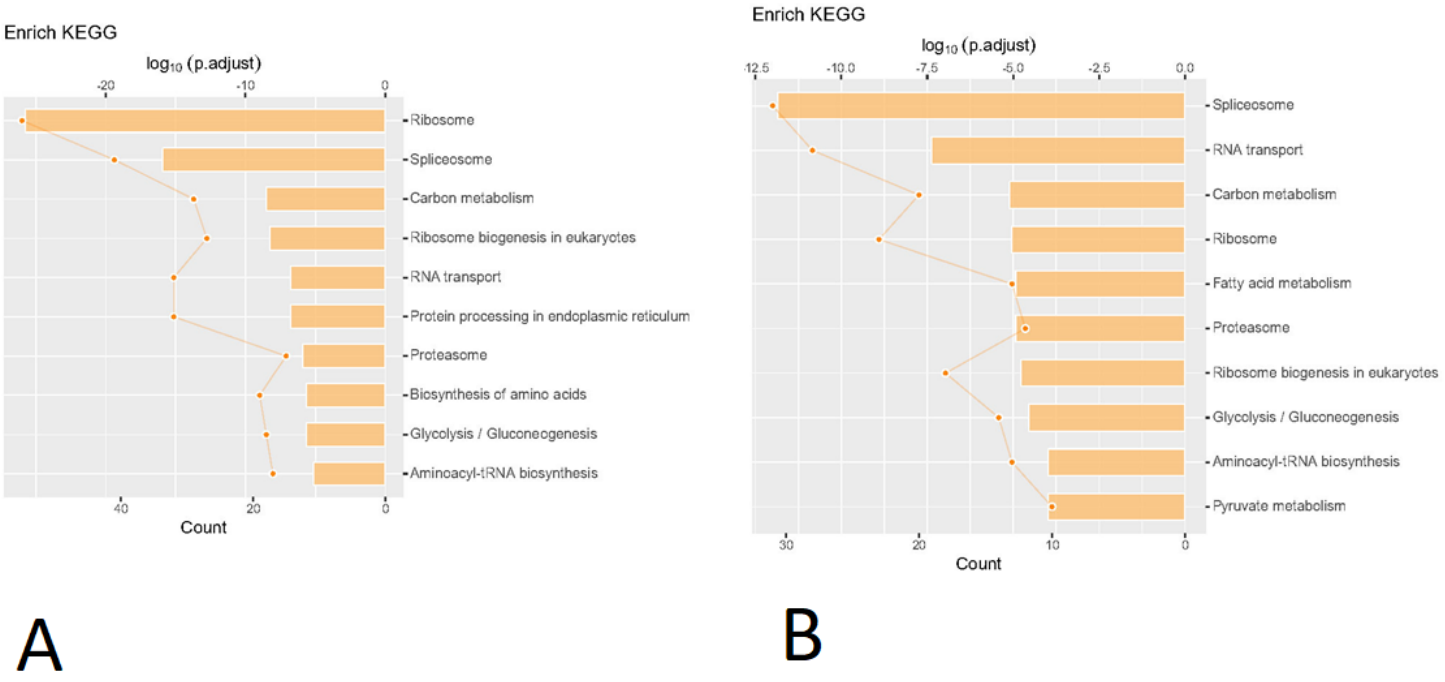

Figure 7

a: Enriched KEGG items of < T > in Control-A549 vs. IgG-A549, if no protein matched or less than 5 enriched items found, on plot will be displayed. b. Enriched KEGG items of < T > in LPS-A549 vs. IgG-LPS, if no protein matched or less than 5 enriched items found, on plot will be displayed.

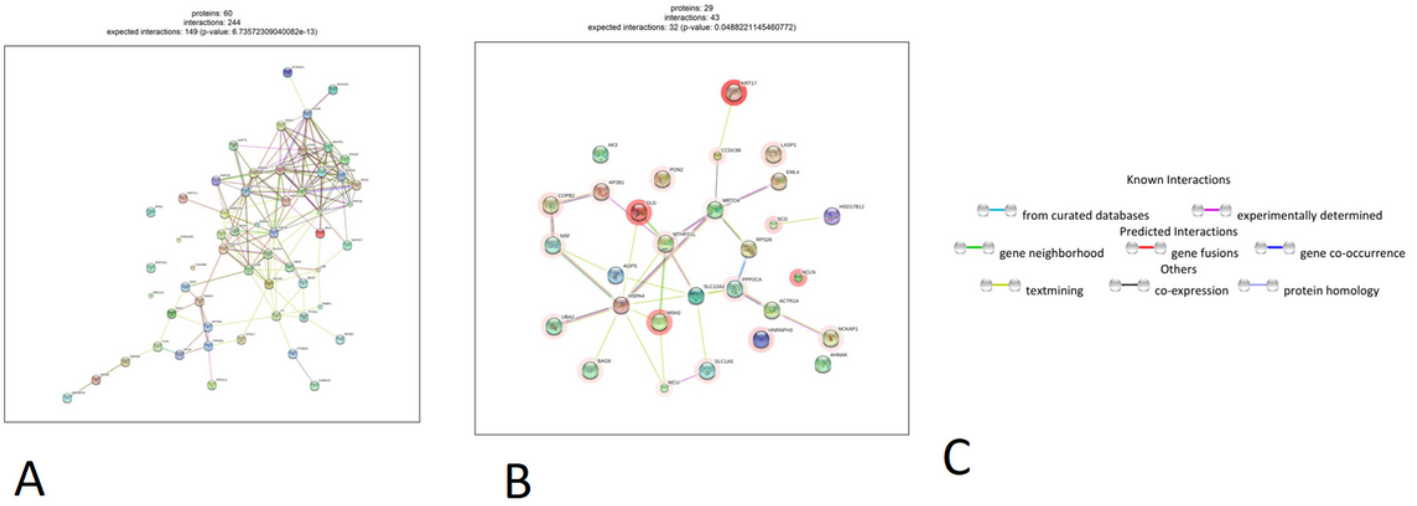

Figure 8

a. STRING protein-protein interaction analysis. Protein interaction analysis of control-A549 specifically enriched proteins by STRINGdb showed that there were 244 significant enriched interactions among 60 proteins. (p-value: 6.73572309040082e-13) b. STRING protein-protein interaction analysis. Protein interaction analysis of LPS-A549 specifically enriched proteins by STRINGdb showed that there were 43 significant enriched interactions among 29 proteins. (p-value: 0.0488221145460772) c. Edge color legends. The explanation of protein-protein interaction links. It is divided into two parts: known interactions and predicted interactions.C

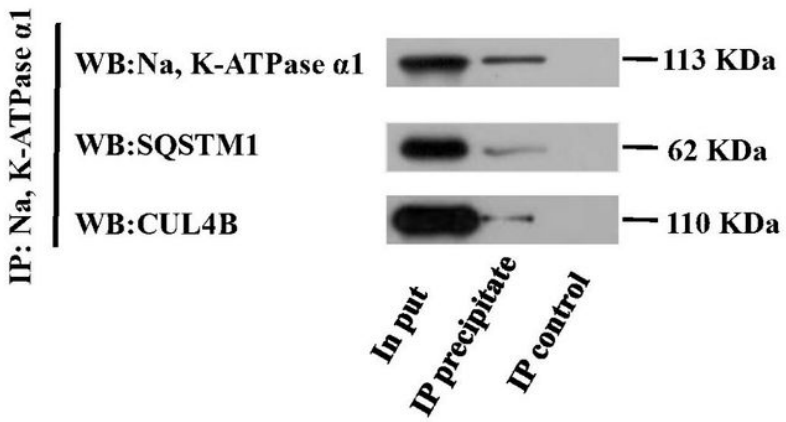

Figure 9

The binding of Na, K-ATPase α1 to SQSTM1 and CUL4B were verified by endogenous Co-IP. Proteins in whole-cell lysate were used as a positive control (Input). IP: Na, K-ATPase murine monoclonal antibody, abcam□ab2872. Na, K-ATPase α1 group, WB: 1:1000, 100KD. Second antibody: Goat anti-Mouse IgG (Light Chain Specific), HRP Conjugated, S003, 1:5000. SQSTM1 group, WB: SQSTM1 rabbit polyclonal antibody, Proteintech, 18420-1, 1:10000, 62KD; Second antibody: Mouse anti-Rabbit IgG (Light Chain specific), HRP Conjugated, S006, 1:5000. CUL4B group, WB: CUL4B rabbit polyclonal antibody, Immunoway, YM5188, 1:1000, 110KD; Second antibody: Mouse anti-Rabbit IgG (Light Chain specific), HRP Conjugated, S006, 1:5000.62KD.

Supplementary Files

This is a list of supplementary files associated with this preprint. Click to download.

- SupportingInformation.pdf